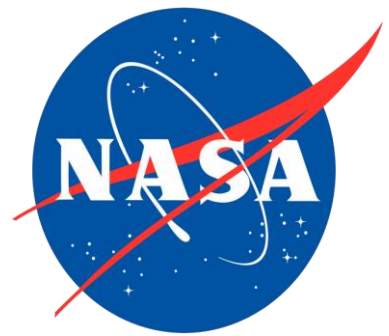


Andréa Hughes<sup>1</sup>, Michael Chaffin<sup>2</sup>, Edwin Mierkiewicz<sup>1</sup>, J. Deighan<sup>2</sup>, J.Y. Chaufray<sup>3</sup>, N.M. Schneider<sup>2</sup>, E. Thiemann<sup>2</sup>, J.T. Clarke<sup>4</sup>, M. Mayyasi<sup>4</sup>, S.K. Jain<sup>2</sup>, M.M.J. Crismani<sup>2</sup>, A. Stiepen<sup>5</sup>, F. Montmessin<sup>3</sup>, F. G. Eparvier<sup>2</sup>, A.I.F. Stewart<sup>2</sup>, W.E. McClintock<sup>2</sup>, G.M. Holsclaw<sup>2</sup>, B.M. Jakosky<sup>2</sup>

(1) Department of Physical Sciences, Embry-Riddle Aeronautical University, Daytona Beach, FL, (2) Laboratory for Atmospheric and Space Physics, University of Colorado Boulder, Boulder, Colorado, USA, (3) LATMOS/IPSL, Guyancourt, Yvelines/Île-de-France, Guyancourt, France, (4) Center for Space Physics, Boston University, Boston, Massachusetts, USA, (5) Laboratoire de Physique Atmosphérique et Planétaire (LPAP) Université de Liège, Liège, Belgium

Contact E-mail: ACGHughes@gmail.com



## I. Introduction and Background

Proton Aurora: a third type of aurora (in addition to diffuse and discrete) newly identified at Mars

- Formed by penetrating protons from solar wind charge exchange
- Not constrained by a global magnetic field
- Expected to occur only on Mars' dayside

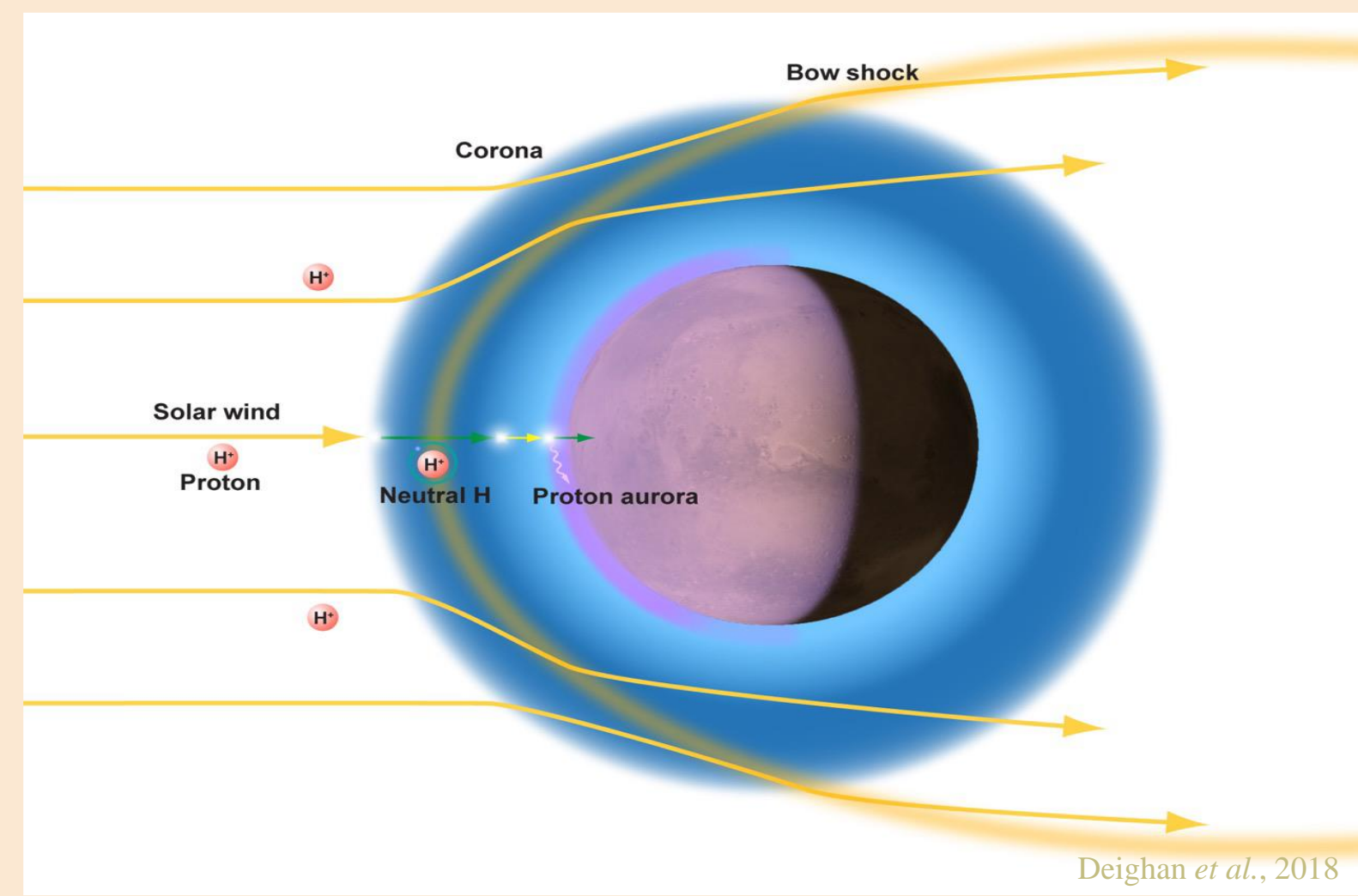


Figure 1: Mechanism for Martian proton aurora originating from solar wind charge exchange (Deighan et al., 2018)

### Project Goals:

- Better understand solar wind's interaction with Mars' hydrogen corona
- Create a comprehensive catalog characterizing Martian proton aurora

## II. Data and Methods

Using data from the Imaging UltraViolet Spectrograph (IUVS) onboard the Mars Atmosphere and Volatile Evolution (MAVEN) spacecraft, we evaluate the hydrogen Lyman-alpha emission (121.6 nm) from periapsis limb scans throughout the entire mission (~1.5 Martian years).

### Data Collection and Reduction Process:

1. IUVS limb scans taken during orbit periapse

2. FUV and MUV spectral and spatial data collected; spectral intensity profile created

3. Data corrected by subtracting background Ly- $\alpha$ , applying flat field, and KR conversion.

4. Altitude profile created by summing intensities under Ly- $\alpha$  curve (one point for each mirror position and slit position); data binned by altitude

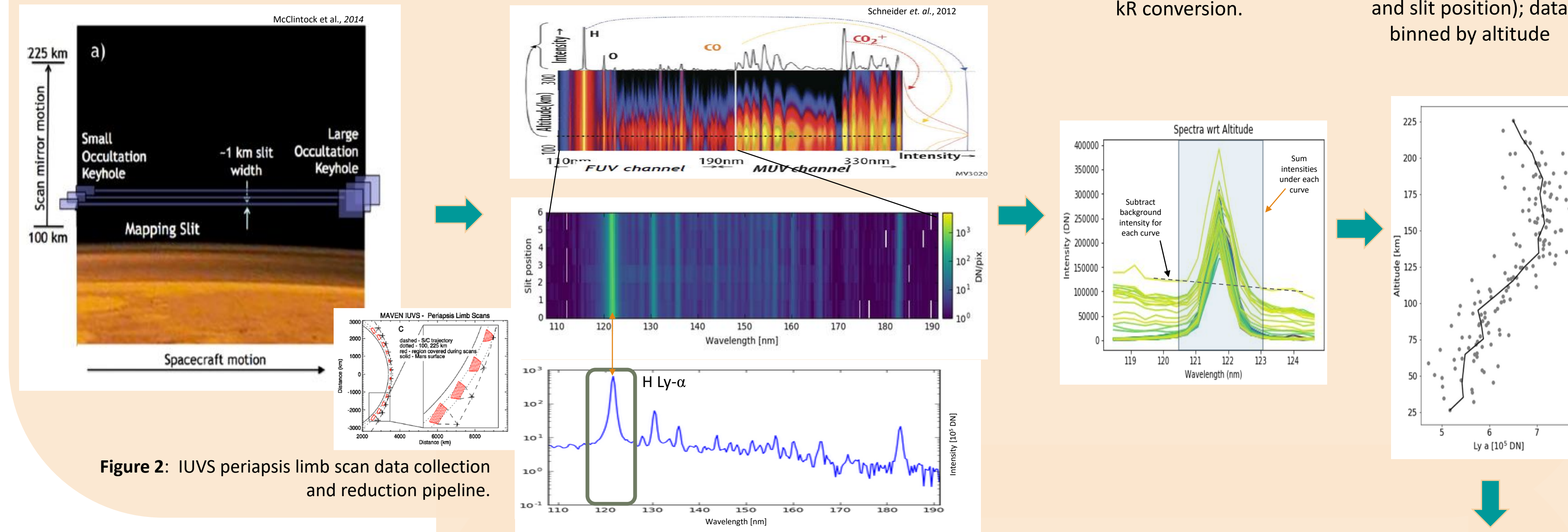


Figure 2: IUVS periapsis limb scan data collection and reduction pipeline.

## III. Observations

• Proton aurora events correlated with low SZA's, high intensities, and large peak enhancements (A & B)

• Proton aurora observed only on day side of planet (apparent "exceptions" occur at high latitudes and/or near summer) (C)

• Highest intensities, emission enhancements, and frequency of events occur near S. Summer solstice ( $L_s = 270$ ) (E & F)

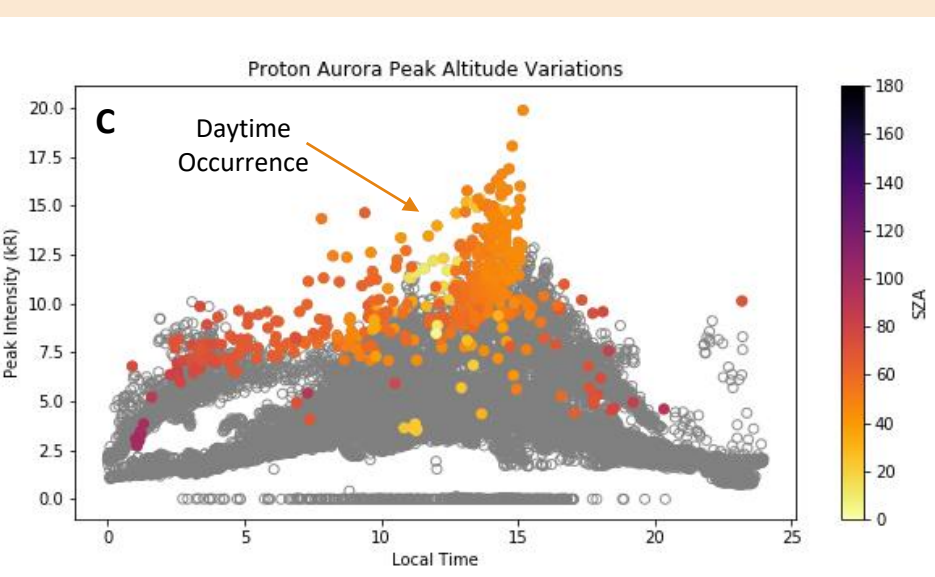


Figure 6A: Proton Aurora Peak Altitude Variations (Global)

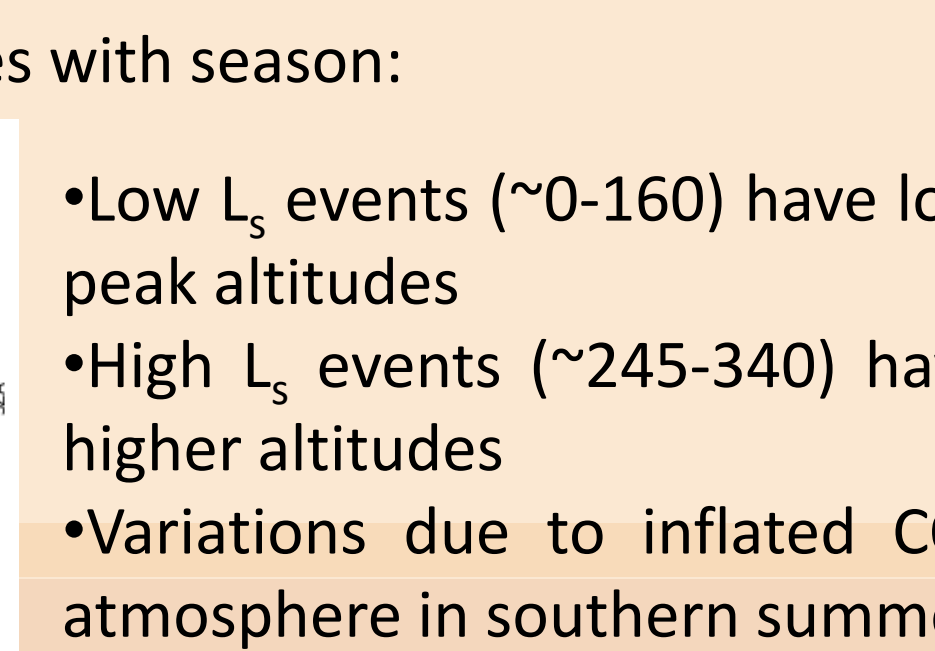


Figure 6B: Proton Aurora Peak Altitude Variations (Global)

Figure 6C: Proton Aurora Peak Altitude Variations (Daytime Occurrence)

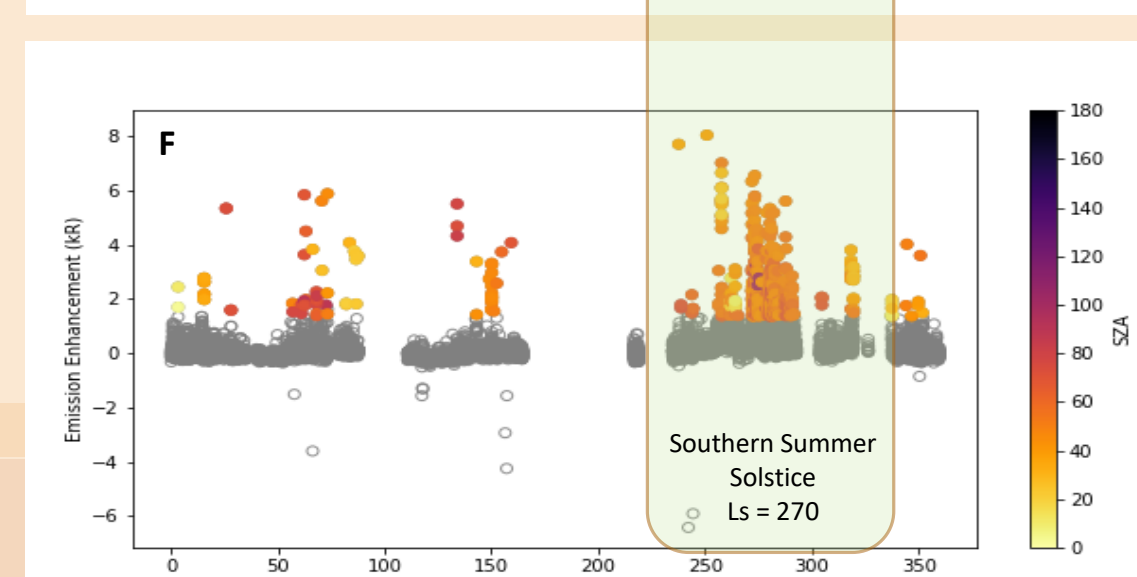
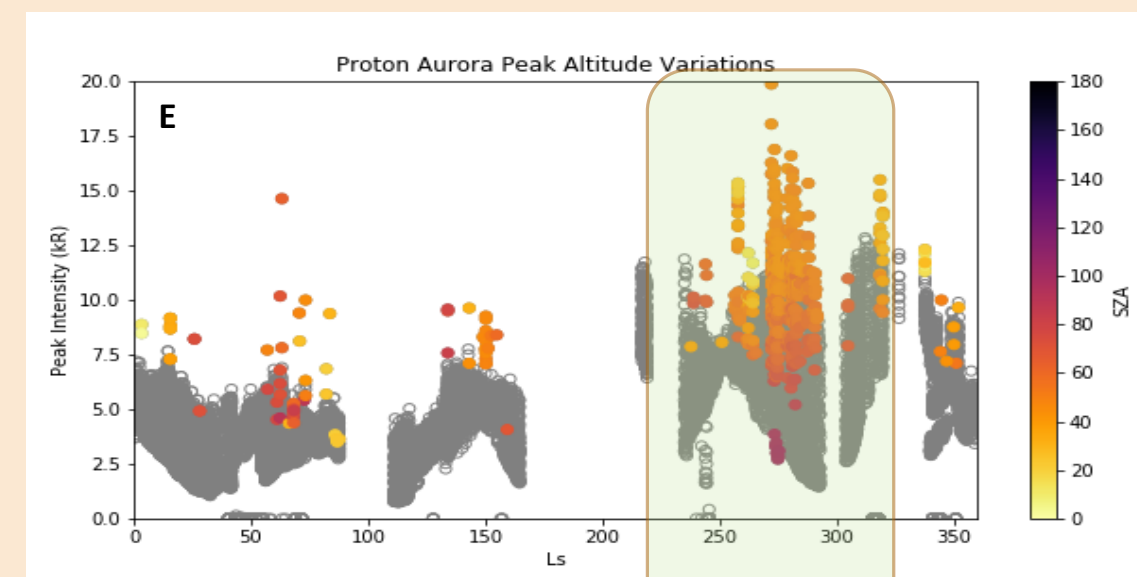


Figure 6F: Proton Aurora Peak Altitude Variations (Southern Summer Solstice)

Altitude of peak enhancement varies with season:

- Low  $L_s$  events ( $\sim 0-160$ ) have low peak altitudes
- High  $L_s$  events ( $\sim 245-340$ ) have higher altitudes
- Variations due to inflated  $CO_2$  atmosphere in southern summer

Figure 6 (A-F): Variations in proton aurora events. Proton aurora detections (colored) overlain on non-detections (grey).

Proton aurora exhibit enhanced brightness peak between  $\sim 120-150$  km altitude (e.g., June 2015 & Nov. 2016 in Fig. 3)

Figure 3: Top: Profiles of maximum, minimum, and median (at 150 km altitude) for select months; color corresponds to SZA & solid lines are binned averages. Bottom: Ly- $\alpha$  Intensities and SZA's for all orbits.

### Detection Method: "Global statistic Method"

- 1) Separate data into peak and high altitude regions
- 2) Difference: 2<sup>nd</sup> highest peak alt intensity – median high alt intensity
- 3) Threshold: standard deviation of differences of entire dataset (e.g.  $3\sigma$  in this study).

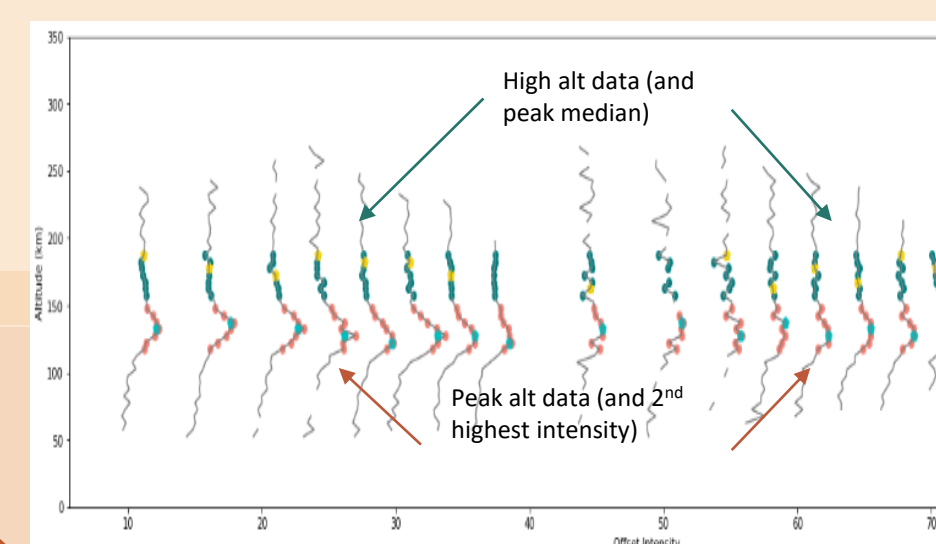


Figure 4: (left) Example of data used in step 1 and step 2 of detection method

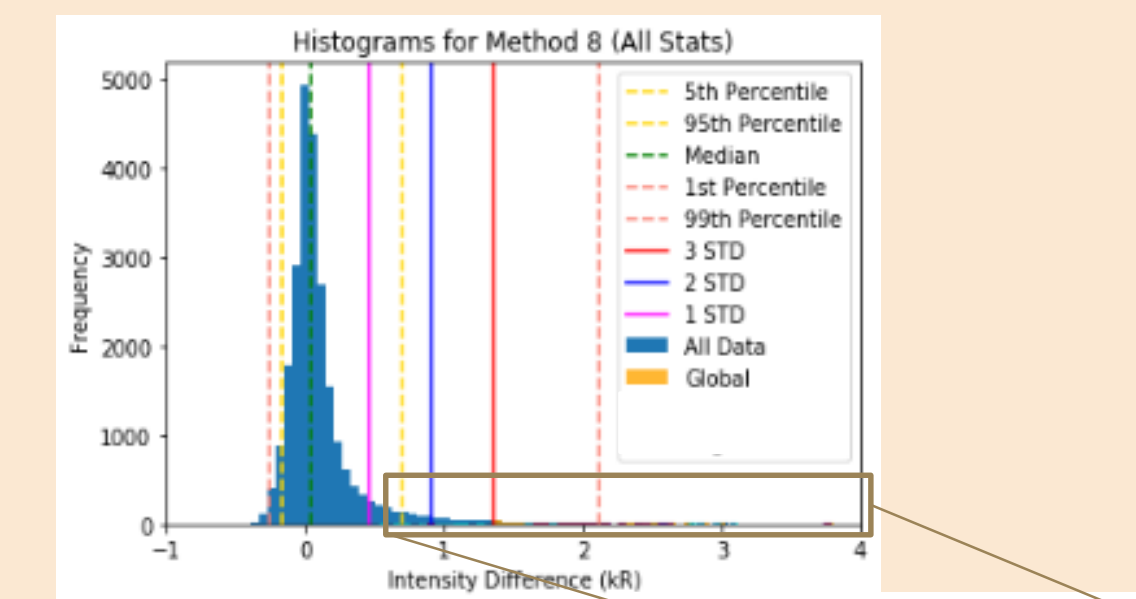


Figure 5: Graphic Representation of step 3 in detection method. Histogram shows intensity differences of all data (top left); proton aurora detections display enhancements exceeding the  $3\sigma$  threshold (top right).

## IV. Summary and Conclusions

- Using current rigorous detection constraints ( $3\sigma$  threshold), we identify **486 individual profiles exhibiting definite proton aurora events, from 137 unique orbits** (only 9 detections reported prior)
- May be **more common than previously thought** (definitive proton aurora detections occurring in  $>2\%$  of profiles and  $>5\%$  of orbits)
- Correspond with **low SZA's and occur almost entirely in daytime**
- Some interesting seasonal variations: **peak altitudes, emission enhancements, intensities and frequency of proton aurora events are all higher near S. Summer.**

## V. Outstanding Questions and Future Work

- What are the locations (geographic, temporal, etc.) of proton aurora events at Mars? Is there any interaction with an upstream magnetic field?
- Compare selected altitude profiles to model predictions, possibly via a model challenge

### Acknowledgments

Many thanks to Coauthors, Collaborators, and funding sources, including:  
 • CEDAR Student Travel Funding  
 • John Mather Nobel scholarship  
 • NASA Astrobiology Early Career Collaboration Award  
 • Florida Space Grant Consortium

### References

[1] McClintock et al., 2014 [2] Schneider et al., 2012 [3] Chaffin et al., 2017 [4] Mayyasi et al., 2017 [5] Halekas 2017 [6] Clarke et al., 2017 [7] Bhattacharyya et al., 2017 [8] Jakosky, B. M. et al., 2017 [9] Deighan et al., 2018 (in review) [10] Ritter et al., 2018 [11] Halekas et al. 2015 [12] Vegard, 1939 [13] Eather, 1967